J. Khaliq, C. Li, K. Chen, B. Shi, H. Ye, A.M. Grande, H. Yan, M.J. Reece
Reduced Thermal Conductivity by Nanoscale Intergrowths in Perovskite Like Layered Structure La2Ti2O7
Journal of Applied Physics, Vol. 117, N. 7, 2015, 075101 (7 pages)
doi:10.1063/1.4908209

JOURNAL OF APPLIED PHYSICS 117, 075101 (2015)

Reduced thermal conductivity by nanoscale intergrowths in perovskite like layered structure $La_2Ti_2O_7$

Jibran Khaliq,[1] Chunchun Li,[2] Kan Chen,[1] Baogui Shi,[3] Haitao Ye,[3] Antonio M. Grande,[4] Haixue Yan,[1,5] and Michael J. Reece[1,5,a)]
[1]*School of Engineering and Material Science, Queen Mary University of London, London E1 4NS, United Kingdom*
[2]*Electronic Materials Research Laboratory, Key Laboratory of the Ministry of Education & International Centre for Dielectric Research, Xi'an Jiaotong University, Xi'an, 710049, China*
[3]*School of Engineering and Applied Science, Aston University, Birmingham B4 7ET, United Kingdom*
[4]*Faculty of Aerospace Engineering, Delft University of Technology, Kluyverweg 1, 2629 HS Delft, The Netherlands*
[5]*Nanoforce Technology Limited, London E1 4NS, United Kingdom*

(Received 27 November 2014; accepted 3 February 2015; published online 18 February 2015)

The effect of substitution and oxidation-reduction on the thermal conductivity of perovskite-like layered structure (PLS) ceramics was investigated in relation to mass contrast and non-stoichiometry. Sr (acceptor) was substituted on the A site, while Ta (donor) was substituted on the B site of $La_2Ti_2O_7$. Substitution in PLS materials creates atomic scale disorders to accommodate the non-stoichiometry. High resolution transmission electron microscopy and X ray diffraction revealed that acceptor substitution in $La_2Ti_2O_7$ produced nanoscale intergrowths of $n = 5$ layered phase, while donor substitution produced nanoscale intergrowths of $n = 3$ layered phase. As a result of these nanoscale intergrowths, the thermal conductivity value reduced by as much as ~20%. Pure $La_2Ti_2O_7$ has a thermal conductivity value of ~1.3 W/m K which dropped to a value of ~1.12 W/m K for Sr doped $La_2Ti_2O_7$ and ~0.93 W/m K for Ta doped $La_2Ti_2O_7$ at 573 K. © *2015 AIP Publishing LLC*.
[http://dx.doi.org/10.1063/1.4908209]

INTRODUCTION

Thermoelectrics can convert waste heat into electricity by utilizing the Seebeck effect.[1] They do not possess any moving parts, which make them potentially reliable and long lasting.[2] The efficiency of a thermoelectric material can be represented by a dimensionless figure of merit (zT) which depends on Seebeck coefficient (S), electrical conductivity (σ), and thermal conductivity (κ). Conventional thermoelectric materials, like Bi_2Te_3, skutterudites, and PbTe are classed as efficient thermoelectric materials. Bi_2Te_3 related compounds have a maximum efficiency near room temperature[3] and comparatively low operating temperatures (<200 °C), while skutterudites and PbTe are classed as intermediate temperature thermoelectrics (up to 650 °C).[4–8] These materials are being used in large scale applications but they have high processing costs[9] and use toxic elements. Most of these materials have zT close to unity, but they are not stable in air due to the oxidation at these temperatures.[10]

Oxide materials are inexpensive, abundant in nature, non-toxic, and environmentally friendly. These materials possess high chemical and thermal stability which makes them suitable for high temperature thermoelectric application in air.[11,12] Oxide materials offer great flexibility in structural and compositional variations to alter their thermoelectric properties. $Na_xCo_2O_4$ based oxides have shown some promising results,[13] but toxicity of cobalt and volatility of Na are a concern.

There has been considerable interest recently in $SrTiO_3$ due to its high Seebeck coefficient.[14] $SrTiO_3$ is a perovskite structured compound and the structure of $SrTiO_3$ can be represented by stacks of corner sharing TiO_6 octahedra. $SrTiO_3$ has a thermal conductivity value of ~ 10 W/m K,[15] which is on the higher side for thermoelectric applications. Compared to perovskite phases, layered perovskite structure phases have much larger unit cells which produce lower thermal conductivities.[16] Examples of these kinds of structures are Perovskite-like layered structure (PLS),[17,18] Aurivillius,[19] and Ruddlesden-Popper.[16] They consist of multiple layers of perovskite units separated by systematic layers.[20,21] For this reason, the layered perovskite structured compounds exhibit anisotropic and anomalously low thermal conductivity values compared to the perovskite structured compounds.[20,22] Very low and temperature independent thermal conductivity have been reported for polycrystalline layered perovskite compounds like $Bi_4Ti_3O_{12}$ (~1 W/m K)[21] and $Sr_2Nb_2O_7$ (1.5 W/m K).[23]

$La_2Ti_2O_7$ is the member of the perovskite-like layered structure family with general formula $A_nB_nO_{3n+2}$. The n in the formula represents the number of octahedral units in the perovskite layers, which in the case of $La_2Ti_2O_7$, is four. Its structure consists of corner shared TiO_6 octahedra in the unit cell. Two sets of perovskite layers constitute a unit cell. $La_2Ti_2O_7$ possesses a monoclinic unit cell at room temperature with a space group of $P2_1$ ($a = 13.0150$ Å, $b = 5.5456$ Å, $c = 7.8170$ Å, and $\beta = 98.6°$). It possesses the basic requirements for low thermal conductivity, such as large atomic mass, crystal anisotropy, and a complex structure with the

a)Author to whom correspondence should be addressed. Electronic mail: m.j.reece@qmul.ac.uk Tel.: +44 (0)20 7882 8872.

possibility of inducing disorder.[24] By engineering the microstructure of the layered compounds, the thermal conductivity can be reduced by creating more scattering centres.[25] In this work, we substituted Sr and Ta in $La_2Ti_2O_7$ to create defects inside the microstructure due to mismatch between valence, atomic radii and the atomic weights of the host and the substituted elements.

The objective of this work is to investigate for the first time, the effect of acceptor-donor substitution and oxidation-reduction on the thermal conductivity due to atomic scale defects in $La_2Ti_2O_7$.

EXPERIMENTAL PROCEDURE

$La_2Ti_2O_7$, $La_{1.6}Sr_{0.4}Ti_2O_{6.8\pm\delta}$, and $La_2Ti_{1.7}Ta_{0.3}O_{7.15\pm\delta}$ were prepared by solid state reaction. The starting materials were La_2O_3 (99.99% purity, Sigma Aldrich), $SrCO_3$ (99.9% purity, Sigma Aldrich), TiO_2 (anatase) (99.6% purity, Alfa aesar) and Ta_2O_5 (99.85% purity, Alfa aesar). These powders were mixed in stoichiometric ratios and ball milled using ethanol as a milling medium in a planetary ball mill. Mixed powders were calcined at 1300 °C for 4 h. After calcination, the powders were remilled for 4 h to break the agglomerates and reduce the particle size.

Calcined powders were sintered using a Spark Plasma Sintering (SPS) furnace (HPD 25/1, FCT, Rauenstein, Germany). The powders were cold pressed into a 20 mm graphite die and sintered at 1350 °C under 50 MPa of pressure for 5 min. The vacuum level inside the furnace was ~ 5 Pa. The sintered discs were annealed at 1000 °C for 6 h to remove any carbon contamination. For comparison, the air annealed discs were reduced at 1200 °C for 4 h in a mixture of 10% H_2 and 90% Ar in a laboratory furnace (thermal technology LLC, Model number 1100 2560 1/2). The bulk density was measured by Archimedes principle and presented in Table I. All sintered samples were more than 98% dense.

SAMPLE CHARACTERIZATION

X ray diffraction (XRD) patterns for powders, as sintered, air annealed, and hydrogen reduced samples were obtained using an X-ray diffractometer (Siemens D5000, Karlsruhe, Germany) using CuKα radiation. The microstructures of the ceramic samples were observed using Transmission Electron Microscopy (TEM) Jeol JEM 2010 200KV. All of the ceramics were observed along the pressing direction. The samples for TEM were prepared using a Precision Ion polishing System (PIPS™). Thermal conductivity was calculated using the formula $\kappa = \rho C_p D$, where ρ is the density measured by Archimedes principle, C_p is the specific heat measured using a Netzsch STA (449 F3 Jupiter®), and D is the thermal diffusivity measured using a netszch LFA 457 microflash using 20 mm discs under Ar environment. The thermal diffusivity measurements were repeated to check reproducibility of the measurement. Elastic modulus was measured by Micro Indentation Tester from CSM Instruments (Switzerland) with a 100 μm radius sphere-conical diamond indenter tip. The valence of the elements was determined by the X-ray photoelectron spectroscopy (XPS; ESCALAB MK II, VG Scientific). All the spectra are corrected against the C reference peak at 285 eV for different elements.

TABLE I. Archimede's density for $La_2Ti_2O_7$ based ceramics.

Composition	Density, g/cc
$La_2Ti_2O_{7\pm\delta}$ air annealed	5.74 ± 0.04
$La_2Ti_2O_{7\pm\delta}$ reduced	5.62 ± 0.01
$La_{1.6}Sr_{0.4}Ti_2O_{6.8\pm\delta}$ air annealed	5.53 ± 0.03
$La_{1.6}Sr_{0.4}Ti_2O_{6.8\pm\delta}$ reduced	5.47 ± 0.01
$La_2Ti_{1.7}Ta_{0.3}O_{7.15\pm\delta}$ air annealed	6.07 ± 0.02
$La_2Ti_{1.7}Ta_{0.3}O_{7.15\pm\delta}$ reduced	5.98 ± 0.03

RESULTS AND DISCUSSIONS

The $La_2Ti_2O_7$ was single phase after calcination, sintering, and subsequent heat treatments. The XRD peaks matched the PDF card # 28–0517 (supplementary material[26]). Figure 1(a) shows the X-ray diffraction patterns for $La_{1.6}Sr_{0.4}Ti_2O_{6.8\pm\delta}$. The peaks match with $La_2Ti_2O_7$ ($LaTiO_{3.5}$), n = 4 (PDF card # 28–0517). The peaks were shifted towards lower angles indicating that the lattice parameter increased as a result of substitution of La^{3+} (ionic radius 1.17 Å) by Sr^{2+} (ionic radius 1.32 Å).[27] All the peaks were sharp giving an indication of a large particle size of the powder according to the Scherrer formula.[28] A secondary phase was detected in the calcined powder which could not be indexed and is marked as *. After sintering, the unidentified secondary phase disappeared and a new second phase was produced, which is indicated with the symbol ◆ in Figure 1(a). This new phase was a five layer perovskite phase. After air annealing, the amount of five layer perovskite phase decreased. This effect was reversed slightly during reduction and the amount of five layer perovskite phase increased. This is due to the fact that the five layer perovskite phase is more stable in a low partial pressure of oxygen as it has a smaller oxygen to cation ratio compared to $La_2Ti_2O_7$ (A:B:O is 1:1:3.5 for $La_2Ti_2O_7$ and 1:1:3.4 for $A_5B_5O_{17}$).[29]

Figure 1(b) shows the X ray diffraction patterns for $La_2Ti_{1.7}Ta_{0.3}O_{7.15\pm\delta}$. The peaks matched with $La_2Ti_2O_7$ ($LaTiO_{3.5}$), n = 4 (PDF card # 28-0517). A second phase was also detected as a result of Ta substitution which was a three layer perovskite phase. The three layer perovskite phase has higher oxygen to cation ratio compared to $La_2Ti_2O_7$ (A:B:O is 1:1:3.5 for $La_2Ti_2O_7$ and 1:1:3.7 for $A_3B_3O_{11}$). The amount of five and three layer perovskite phases was estimated by Normalized Relative Intensity Ratio (RIR) method proposed by Chung[30] and is presented in Table II.

Figure 2(a) shows a typical bright field TEM image of the $La_2Ti_2O_7$ based ceramics after air annealing. The typical grain size was ~ 0.7 μm and most of the grains were defect free except for a few planar defects. Figure 2(b) shows a (100) lattice image of $La_2Ti_2O_7$. Figure 2(c) shows a bright field TEM image of $La_{1.6}Sr_{0.4}Ti_2O_{6.8\pm\delta}$ air annealed ceramic, which has a high density of nanoscale intergrowths of five layer perovskite phase inside $La_2Ti_2O_7$. These

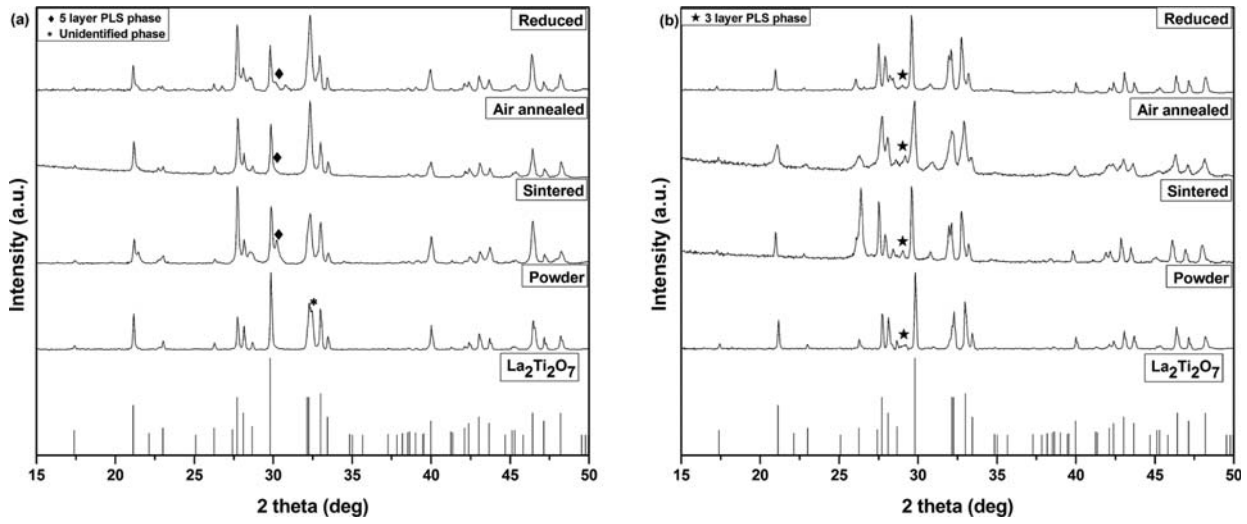

FIG. 1. XRD patterns of (a) $La_{1.6}Sr_{0.4}Ti_2O_{6.8\pm\delta}$ and (b) $La_2Ti_{1.7}Ta_{0.3}O_{7.15\pm\delta}$.

TABLE II. Mass percentage of the secondary phase in Sr and Ta substituted $La_2Ti_2O_7$.

	Powder (mass %)	Sinter (mass %)	Air Annealed (mass %)	Reduced (mass %)
$La_{1.6}Sr_{0.4}Ti_2O_{6.8\pm\delta}$	…	8.4	3.0	7.8
$La_2Ti_{1.7}Ta_{0.3}O_{7.15\pm\delta}$	3.6	4.6	4.6	1.7

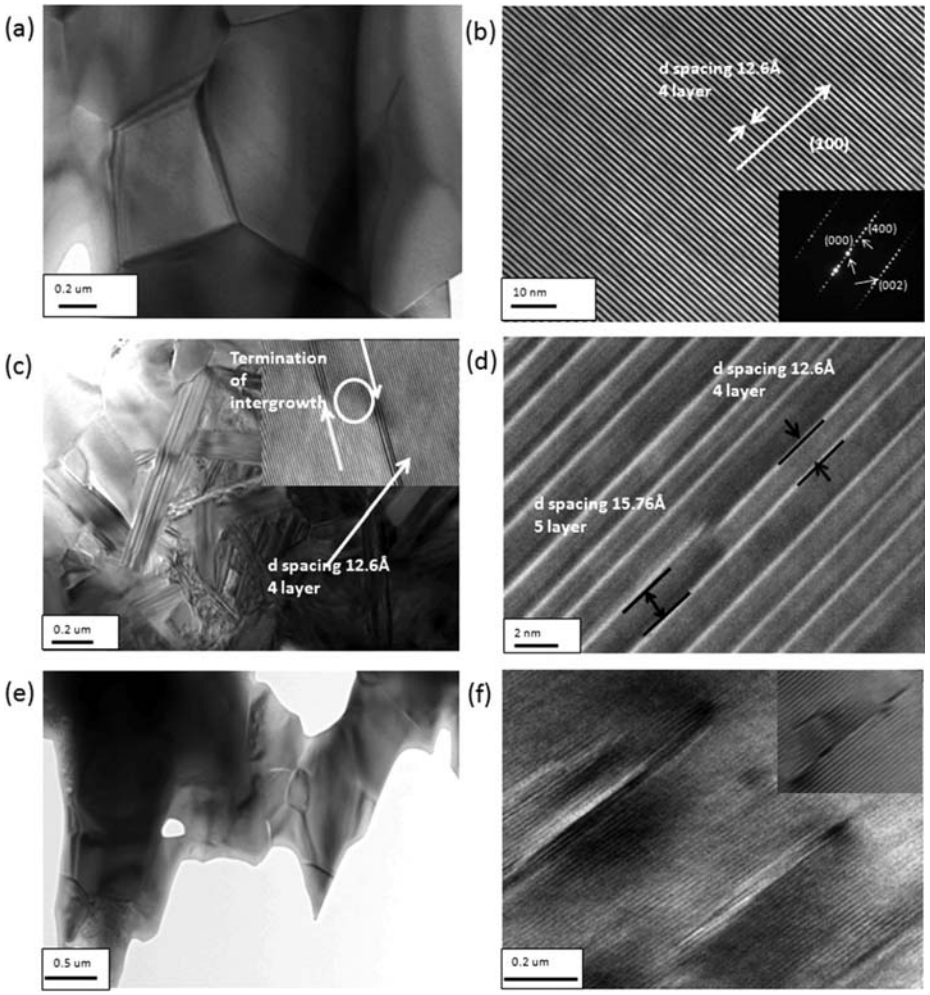

FIG. 2. TEM images of (a) air annealed $La_2Ti_2O_7$; (b) lattice image of air annealed $La_2Ti_2O_7$; (c) air annealed $La_{1.6}Sr_{0.4}Ti_2O_{6.8\pm\delta}$; (d) lattice image of air annealed $La_{1.6}Sr_{0.4}Ti_2O_{6.8\pm\delta}$; (e) air annealed $La_2Ti_{1.7}Ta_{0.3}O_{7.15\pm\delta}$; and (f) lattice image of air annealed $La_2Ti_{1.7}Ta_{0.3}O_{7.15\pm\delta}$.

intergrowths had a $(100)_5 \parallel (100)_4$ epitaxy and were distributed homogeneously throughout the ceramic.[31] Some of the intergrowths terminated or moved to a different plane of the $La_2Ti_2O_7$ as shown in Figure 2(d). When an intergrowth terminated, it disturbed the neighbouring planes as seen in Figures 2(c) and 2(d).

Figure 2(e) shows a bright filed TEM image of $La_2Ti_{1.7}Ta_{0.3}O_{7.15\pm\delta}$ ceramic after air annealing with some planar defects which were distributed homogeneously throughout the ceramic. From XRD data, the formation of three layered perovskite phase was confirmed. So, the regions of planar defects are the regions of three layered perovskite phase embedded inside four layered $La_2Ti_2O_7$. The morphology of the intergrowths in $La_2Ti_{1.7}Ta_{0.3}O_{7.15\pm\delta}$ is different from that in $La_{1.6}Sr_{0.4}Ti_2O_{6.8\pm\delta}$. The intergrowths are shorter and terminate within the 4 layer PLS phase as shown in the inset in Figure 2(f).

Figures 3(a)–3(c) show the XPS spectra of surface electrons for different elements in $La_2Ti_2O_7$ ceramics after ion beam etching. The ion beam etching was done for 5 min. Since the C reference used by different labs varies, the absolute value of each element varies in a range. The binding energy (BE) values for La 3d showed a clear doublet for both components ($La3d_{5/2}$ and $La3d_{3/2}$) which is a characteristic of La containing oxide compounds.[32] The binding energy difference between the splitting of $La3d_{5/2}$ and $La3d_{3/2}$ was ~4.6 eV and ~4.4 eV, respectively, for all of the ceramics. The BE values for Ti 2p showed a clear doublet (Ti $2p_{1/3}$ and Ti $2p_{3/2}$). For air annealed $La_2Ti_2O_7$, the peak position is marked as A (459.17 eV) and the full width half maximum (FWHM) matches the Ti^{4+} state.[33] The Ti $2p_{3/2}$ peak is slightly asymmetric and it gives rise to another peak at 457.67 eV which is marked as B. This peak was caused by the presence of Ti^{3+} state.[34] After reduction, one additional

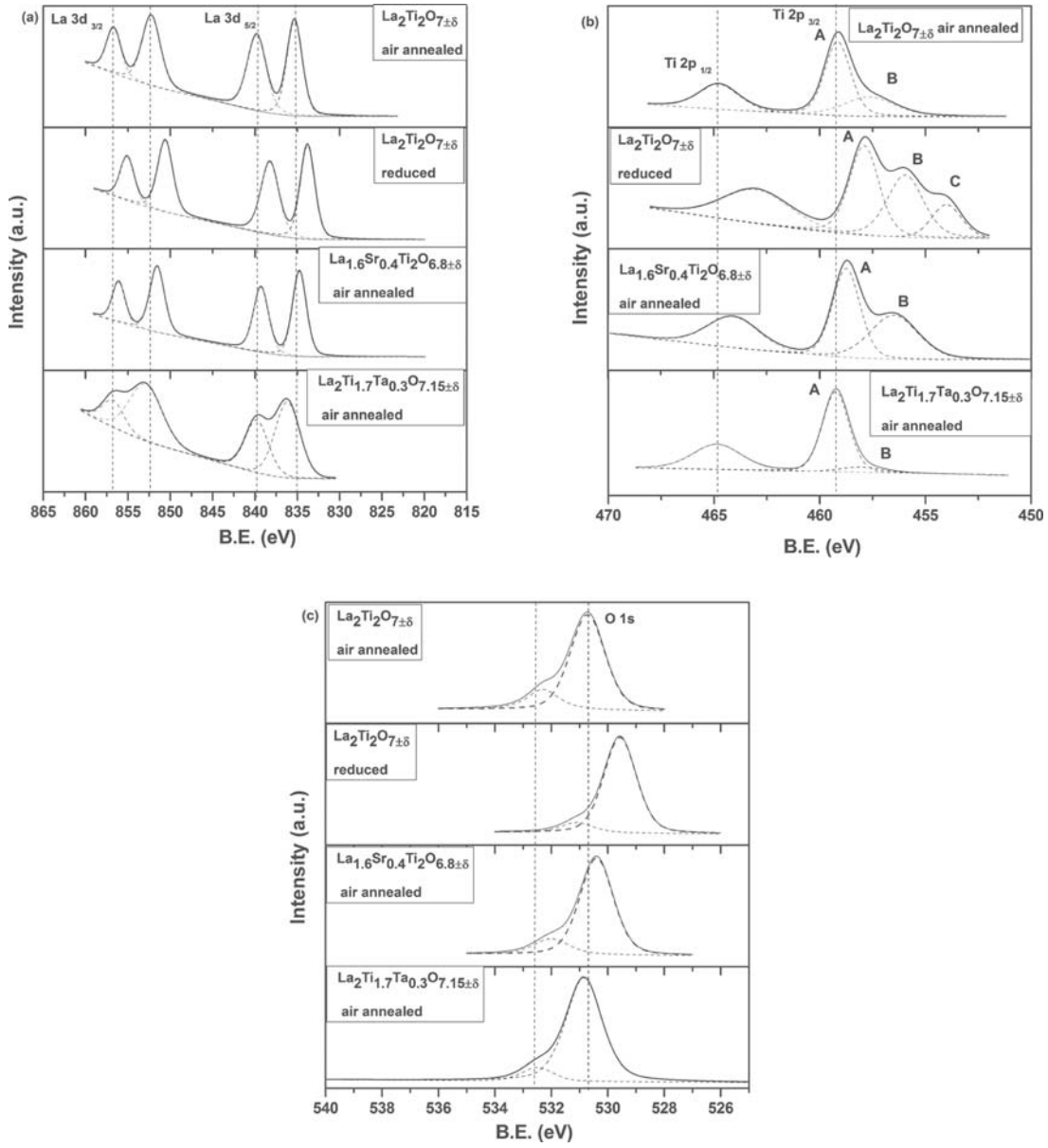

FIG. 3. XPS spectra for $La_2Ti_2O_7$ based ceramics of (a) La 3d; (b) Ti 2p; and (c) O1s.

TABLE III. XPS data of $La_{1.6}Sr_{0.4}Ti_2O_{6.8\pm\delta}$ and $La_2Ti_{1.7}Ta_{0.3}O_{7.15\pm\delta}$ ceramics.

	Peak position (eV)					Binding energy difference (ΔeV)			
	La3d								
Material	$La3d_{3/2}$	$La3d_{5/2}$	Ti2P	O1s	FWHM O 1s	La-O	Ti-O	Sr-O	Ta-O
$La_2Ti_2O_{7\pm\delta}$ air annealed	852.2	835.4	459.2	530.7	1.48	304.7	71.5	…	…
$La_2Ti_2O_{7\pm\delta}$ reduced	850.6	833.8	458	529.6	1.36	304.2	71.6	…	…
$La_{1.6}Sr_{0.4}Ti_2O_{6.8\pm\delta}$ air annealed	851.6	834.8	458.8	530.4	1.38	304.4	71.6	397.0	…
$La_2Ti_{1.7}Ta_{0.3}O_{7.15\pm\delta}$ air annealed	853.0	836.2	459.1	530.7	1.51	305.5	71.6	…	504.4

peak can be seen at 453.9 eV which is marked as C. This peak can be attributed to the Ti^{2+} state as reported in the literature.[35,36] The intensity of the peak marked as B also increased in the reduced ceramic. The B peak which was observed for Ti 2p in pure $La_2Ti_2O_7$ had very low intensity after Ta substitution. All of the O 1s spectra show the same peak symmetry towards the lower binding energy side which can be attributed to the bonded oxygen in the structure as reported in literature.[37] The small higher binding energy peak indicates chemisorbed oxygen or absorbed hydroxyl ions.[32] The FWHMs of the O 1s peak are given in Table III for all the compositions. The FWHM for air annealed $La_2Ti_2O_7$ was 1.48 which decreased to 1.36 after reduction. Sr and Ta substituted $La_2Ti_2O_7$ gave interesting results; the FWHM for O 1s of $La_{1.6}Sr_{0.4}Ti_2O_{6.8\pm\delta}$ and $La_2Ti_{1.7}Ta_{0.3}$ $O_{7.15\pm\delta}$ were 1.38 and 1.51, respectively. This change in FWHM supports the fact that the Sr and Ta substitution in $La_2Ti_2O_7$ produced nanoscale intergrowths (five layer and three layer PLS compounds, respectively) which have different oxygen to cation ratio compared to $La_2Ti_2O_7$ (A:B:O is 1:1:3.5 for $La_2Ti_2O_7$, A:B:O is 1:1:3.4 for $A_5B_5O_{17}$, and 1:1:3.7 for $A_3B_3O_{11}$).

In order to improve the quantitative analysis of the XPS data, the binding energy difference (ΔBE) method was used to reduce scatter in the data[38] and to enable better comparison with the literature. The ΔBE for the pure and Sr/Ta substituted $La_2Ti_2O_{7\pm\delta}$ is given in Table III. The ΔBE for Ti-O for air annealed and hydrogen reduced $La_2Ti_2O_{7\pm\delta}$ samples was calculated to be 71.5 eV and 71.6 eV, respectively. These values are in good agreement with the published literature.[35] The ΔBE for La-O for air annealed $La_2Ti_2O_7$ was found to be 304.7 eV which decreased to 304.2 eV after reduction. This decrease in binding energy was due to a decrease in bonding strength as a result of oxygen removal after reduction. The ΔBE for Ti-O did not change after the addition of Sr. After Sr substitution, the ΔBE for La-O was 304.4 eV which was lower than the pure air annealed $La_2Ti_2O_7$ but higher than the pure reduced $La_2Ti_2O_{7\pm\delta}$. Since La-O bonds are weaker than Ti-O bonds (bond strengths are reported in Ref. 39),[39] the ΔBE results for La-O and Ti-O bonds suggest the presence of localised planar defects/intergrowths in the reduced and Sr substituted $La_2Ti_2O_7$ caused further weakening of the La-O bonds.[40] This also proves the stability of Ti-O bonds in the PLS compounds as a result of substitution/heat treatment. ΔBE for Sr-O was calculated to be 397 eV and it agrees with the reported value.[41]

Based on the microstructural characterization of partially substituted $La_2Ti_2O_7$, it is interesting to study the effect of nanoscale intergrowths on the thermal conductivity. Figure 4(a) shows the thermal conductivity of air annealed $La_2Ti_2O_7$ based ceramics. The thermal conductivity of $La_2Ti_2O_7$ is nearly temperature independent as reported in the literature for similar PLS compounds ($Sr_2Nb_2O_7$).[23] The thermal conductivity for $La_2Ti_2O_7$ was ~1.3 W/m K in this work, which was close to that of other layered structured compounds, e.g., $Bi_4Ti_3O_{12}$ (~1 W/m K).[21] After Sr substitution, the thermal conductivity increased with increasing temperature. The thermal conductivity of $La_2Ti_{1.7}Ta_{0.3}$ $O_{7.15\pm\delta}$ ceramics is nearly temperature independent like $La_2Ti_2O_7$ and decreased with Ta substitution. Figure 4(b) shows the thermal conductivity of reduced $La_2Ti_2O_7$ based ceramics. After reduction, the values of thermal conductivity for $La_2Ti_2O_{7\pm\delta}$ and $La_{1.6}Sr_{0.4}Ti_2O_{6.8\pm\delta}$ ceramic decreased as compared to the corresponding air annealed sample and the value was less temperature dependent. This decrease in thermal conductivity was caused by the increased amount of nanoscale intergrowths inside the structure as indicated by the TEM and XRD (Table II). While in the case of $La_2Ti_{1.7}$

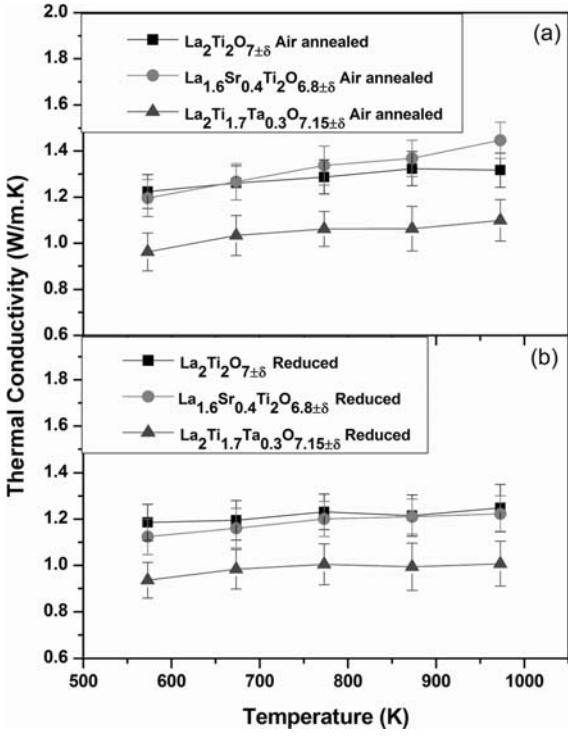

FIG. 4. Variation in thermal conductivity of pure and substituted $La_2Ti_2O_7$ (a) air annealed and (b) reduced.

TABLE IV. Thermal data for $La_2Ti_2O_7$ based ceramics at 973 K.

Composition	Formula mass (amu)	Mean atomic volume (nm^3)	Elastic modulus (GPa)	Theoretical density (g/cc)	Theoretical thermal conductivity (W/m K)	Experimental thermal conductivity (W/m K)
$La_2Ti_2O_{7\pm\delta}$ reduced	485.54	0.01270	200 ± 5	5.78	1.33	1.25 ± 0.07
$La_{1.6}Sr_{0.4}Ti_2O_{6.8\pm\delta}$ reduced	461.83	0.01270	210 ± 5	5.54	1.38	1.22 ± 0.08
$La_2Ti_{1.7}Ta_{0.3}O_{7.15\pm\delta}$ reduced	527.86	0.01310	185 ± 4	6.29	1.24	1.00 ± 0.09

$Ta_{0.3}O_{7.15\pm\delta}$, the value of thermal conductivity decreased only slightly compared to the corresponding air annealed sample.

In order to study the effect of compositional non-stoichiometry on the thermal conductivity, the electronic contribution of thermal conductivity was calculated using the Wiedemann–Franz law to separate its contribution from the lattice thermal conductivity. The Wiedemann–Franz law is given by

$$\kappa_{elec} = LT\sigma, \tag{1}$$

where κ_{elec} is the electronic contribution of thermal conductivity, L is the Lorenz number, T is the absolute temperature, and σ is the electrical conductivity. The value of L was taken from literature as 2.44×10^{-8} W Ω K^{-2} at 573 K.[42] Electrical conductivity was measured using the four probe method in vacuum with laboratory built equipment[43] and was estimated to be ~0.5 S/m for $La_{1.6}Sr_{0.4}Ti_2O_{6.8\pm\delta}$. This had the highest electrical conductivity measured for the substituted PLS ceramics in this work. Based on these values, the κ_{elec} for $La_2Ti_2O_7$ based compositions was estimated to be $<7 \times 10^{-9}$ W/m K, which is very low and it can be concluded that the changes in thermal conductivity were mainly due to the changes in lattice thermal conductivity.[44]

There are potentially two main mechanisms that could influence the thermal conductivity of $La_2Ti_2O_7$ in the present study, mass contrast, and the effect of the nanoscale intergrowths generated as the result of substitution. The effect of change in atomic mass on the thermal conductivity is given by the expression[45]

$$\kappa_{min} = 0.87k_B\Omega^{-2/3}\left(\frac{E}{\rho}\right)^{1/2}, \tag{2}$$

where E is the elastic modulus, ρ is the density, and Ω is the average atomic volume, and k_B is the Boltzmann's constant. The estimated minimum thermal conductivity values are presented in Table IV.

The average atomic volume for $La_2Ti_2O_7$ based compositions was calculated using the following relation and tabulated in Table IV (Ref. 46)

$$\Omega = \frac{M}{m\rho N_A}, \tag{3}$$

where M is the average molar mass of the unit cell, m is the number of atoms per formula unit, ρ is the density, and N_A is the Avogadro's number.

From the above two expressions, it is evident that large mean atomic mass and low elastic modulus favour low thermal conductivity. The atomic masses of $La_2Ti_2O_7$ based compositions are given in Table IV. It is evident from the Table IV that after substitution the atomic mass decreases in the case of $La_{1.6}Sr_{0.4}Ti_2O_{6.8\pm\delta}$ and increases in the case of $La_2Ti_{1.7}Ta_{0.3}O_{7.15\pm\delta}$ compared to pure $La_2Ti_2O_7$. After substituting the elastic modulus (E), the thermal conductivity will increase slightly in the case of $La_{1.6}Sr_{0.4}Ti_2O_{6.8\pm\delta}$ and decrease in the case of $La_2Ti_{1.7}Ta_{0.3}O_{7.15\pm\delta}$. These values hold true for the defect free crystals, but in the case of substituted $La_2Ti_2O_7$, a high density of nanoscale intergrowths was found in the microstructure. Therefore, the thermal conductivity depends on both, the atomic mass difference and the nanoscale intergrowths. This would explain why the experimental thermal conductivities were lower than the minimum theoretical thermal conductivities. This decrease in thermal conductivity by substituting different elements can be explained by the fact that substituted elements produce nanoscale intergrowths in the structure to accommodate non-stoichiometry. The phonons are scattered by these nanoscale intergrowths, thus reducing the thermal conductivity compared to the pure compound (and theoretical minimum thermal conductivity values).

In order to estimate the effect of nanoscale intergrowths/secondary phase on thermal conductivity, the difference between the theoretical thermal conductivity (given in Table IV) and the experimental thermal conductivity was calculated. This difference was negligible in the case of the pure compound. However, the difference increased up to ~20% in the substituted compositions.

CONCLUSION

The effect of acceptor/donor substitution and oxidation-reduction was studied on $La_2Ti_2O_7$. High resolution TEM and XRD revealed that acceptor doping of $La_2Ti_2O_7$ produced nanoscale intergrowth regions of n = 5 layered phase inside n = 4 layered phase, while donor doping produced nanoscale intergrowth regions of n = 3 layered structure. Reduction increased the density of nanoscale intergrowths in Sr substituted $La_2Ti_2O_7$, while it decreased them in Ta substituted $La_2Ti_2O_7$. These nanoscale intergrowths and mass contrast affected the thermal conductivity of substituted $La_2Ti_2O_7$. The thermal conductivity decreased with the increasing amount of nanoscale intergrowths that were generated to accommodate compositional non-stoichiometry. A ~20% decrease in the thermal conductivity was achieved due to the nanoscale intergrowths. A very low thermal conductivity value of ~0.93 W/m K was observed in Ta substituted $La_2Ti_2O_7$ at 573 K. These results suggest that nanoscale intergrowths can effectively reduce the thermal

conductivity of layered perovskites and thus improve their thermoelectric properties. This approach can also be applied to other layered perovskite compounds. For example, the deviation in stoichiometry produced by the substitution of Sr by a higher valence element, such as La in $SrTiO_3$, could be accommodated by the formation of nanoscale intergrowths of layered perovskites.

ACKNOWLEDGMENTS

The authors would like to thank Dr. Na Ni of Imperial College of London, UK and Mr. Samuel Jackson of University of Manchester, UK.

[1]P. Vaqueiro, G. Guelou, M. Stec, E. Guilmeau, and A. V. Powell, J. Mater. Chem. A **1**, 520 (2013).
[2]C. D. Kramer, *Thermoelectric Materials—New Directions and Approaches* (Materials Research Society, 1997), Vol. 478, p. 309.
[3]Q. H. Jiang, H. X. Yan, J. Khaliq, H. P. Ning, S. Grasso, K. Simpson, and M. J. Reece, J. Mater. Chem. A **2**, 5785 (2014).
[4]J. Khaliq, Q. Jiang, J. Yang, K. Simpson, H. Yan, and M. J. Reece, Scr. Mater. **72–73**, 63 (2014).
[5]W. Xie, J. He, H. J. Kang, X. Tang, S. Zhu, M. Laver, S. Wang, J. R. Copley, C. M. Brown, Q. Zhang, and T. M. Tritt, Nano Lett. **10**, 3283 (2010).
[6]J. J. Shen, L. P. Hu, T. J. Zhu, and X. B. Zhao, Appl. Phys. Lett. **99**, 124102 (2011).
[7]J. P. Heremans, V. Jovovic, E. S. Toberer, A. Saramat, K. Kurosaki, A. Charoenphakdee, S. Yamanaka, and G. J. Snyder, Science **321**, 554 (2008).
[8]X. Y. Li, L. D. Chen, J. F. Fan, W. B. Zhang, T. Kawahara, and T. Hirai, J. Appl. Phys. **98**, 083702 (2005).
[9]D. H. Kim, C. Kim, K.-C. Je, G. H. Ha, and H. Kim, Acta Mater. **59**, 4957 (2011).
[10]H. Bando, K. Koizumi, Y. Oikawa, K. Daikohara, V. A. Kulbachinskii, and H. Ozaki, J. Phys.: Condens. Matter **12**, 5607 (2000).
[11]D. Flahaut, T. Mihara, R. Funahashi, N. Nabeshima, K. Lee, H. Ohta, and K. Koumoto, J. Appl. Phys. **100**, 084911 (2006).
[12]C. Yu, M. L. Scullin, M. Huijben, R. Ramesh, and A. Majumdar, Appl. Phys. Lett. **92**, 191911 (2008).
[13]I. Terasaki, Physica B **328**, 63 (2003).
[14]H. Ohta, S. Kim, Y. Mune, T. Mizoguchi, K. Nomura, S. Ohta, T. Nomura, Y. Nakanishi, Y. Ikuhara, M. Hirano, H. Hosono, and K. Koumoto, Nature Mater. **6**, 129 (2007).
[15]H. Muta, K. Kurosaki, and S. Yamanaka, J. Alloys Compd. **392**, 306 (2005).
[16]A. Chernatynskiy, R. W. Grimes, M. A. Zurbuchen, D. R. Clarke, and S. R. Phillpot, Appl. Phys. Lett. **95**, 161906 (2009).
[17]F. Lichtenberg, A. Herrnberger, and K. Wiedenmann, Prog. Solid State Chem. **36**, 253 (2008).
[18]H. Yan, H. Ning, Y. Kan, P. Wang, and M. J. Reece, J. Am. Ceram. Soc. **92**, 2270 (2009).
[19]H. X. Yan, H. T. Zhang, Z. Zhang, R. Ubic, and M. J. Reece, J. Eur. Ceram. Soc. **26**, 2785 (2006).
[20]A. Sakai, T. Kanno, K. Takahashi, A. Omote, H. Adachi, Y. Yamada, and X. D. Zhou, J. Am. Ceram. Soc. **95**, 1750 (2012).
[21]Y. Shen, D. R. Clarke, and P. A. Fuierer, Appl. Phys. Lett. **93**, 102907 (2008).
[22]A. Sakai, T. Kanno, K. Takahashi, Y. Yamada, and H. Adachi, J. Appl. Phys. **108**, 103706 (2010).
[23]T. D. Sparks, P. A. Fuierer, and D. R. Clarke, J. Am. Ceram. Society **93**, 1136 (2010).
[24]D. R. Clarke, Surf. Coat. Technol. **163–164**, 67 (2003).
[25]G. Kieslich, U. Burkhardt, C. S. Birkel, I. Veremchuk, J. E. Douglas, M. W. Gaultois, I. Lieberwirth, R. Seshadri, G. D. Stucky, Y. Grin, and W. Tremel, J. Mater. Chem. A **2**, 13492 (2014).
[26]See supplementary material at http://dx.doi.org/10.1063/1.4908209 for XRD pattern of unsubstituted $La_2Ti_2O_7$.
[27]R. Shannon, Acta Crystallogr., Sect. A **32**, 751 (1976).
[28]P. Scherrer, Nachr. Ges. Wiss. Göttingen, Math. - Phys. Kl. **2**, 98 (1918).
[29]T. Williams, H. Schmalle, A. Reller, F. Lichtenberg, D. Widmer, and G. Bednorz, J. Solid State Chem. **93**, 534 (1991).
[30]F. H. Chung, J. Appl. Crystallogr. **8**, 17 (1975).
[31]S. Lee, J. A. Bock, S. Trolier-McKinstry, and C. A. Randall, J. Eur. Ceram. Soc. **32**, 3971 (2012).
[32]V. V. Atuchin, T. A. Gavrilova, J. C. Grivel, and V. G. Kesler, J. Phys. D: Appl. Phys. **42**, 035305 (2009).
[33]Z. P. Gao, H. X. Yan, H. P. Ning, R. Wilson, X. Y. Wei, B. Shi, H. Ye, and M. J. Reece, J. Eur. Ceram. Soc. **33**, 1001 (2013).
[34]S. Hashimoto and A. Tanaka, Surf. Interface Anal. **34**, 262 (2002).
[35]L. Bugyi, A. Berkó, L. Óvári, A. M. Kiss, and J. Kiss, Surf. Sci. **602**, 1650 (2008).
[36]W. S. Oh, C. Xu, D. Y. Kim, and D. W. Goodman, J. Vac. Sci. Technol. A **15**, 1710 (1997).
[37]Z. Gao, H. Ning, C. Chen, R. Wilson, B. Shi, H. Ye, H. Yan, M. J. Reece, and J. L. Jones, J. Am. Ceram. Soc. **96**, 1163 (2013).
[38]V. V. Atuchin, T. A. Gavrilova, J. C. Grivel, and V. G. Kesler, Surf. Sci. **602**, 3095 (2008).
[39]P. Trocellier, Ann. Chim. Sci. Matér. **25**, 321 (2000).
[40]C. Shi, Z. S. Zhang, M. Crocker, L. Xu, C. Y. Wang, C. T. Au, and A. M. Zhu, Catal. Today **211**, 96 (2013).
[41]V. V. Atuchin, J. C. Grivel, A. S. Korotkov, and Z. Zhang, J. Solid State Chem. **181**, 1285 (2008).
[42]S. R. Popuri, A. J. M. Scott, R. A. Downie, M. A. Hall, E. Suard, R. Decourt, M. Pollet, and J. W. G. Bos, RSC Adv. **4**, 33720 (2014).
[43]G. Li, J. Y. Yang, Y. Xiao, L. W. Fu, J. Y. Peng, Y. Deng, P. W. Zhu, and H. X. Yan, J. Electron. Mater. **42**, 675 (2013).
[44]S. Ohta, T. Nomura, H. Ohta, and K. Koumoto, J. Appl. Phys. **97**, 034106 (2005).
[45]M. R. Winter and D. R. Clarke, J. Am. Ceram. Soc. **90**, 533 (2007).
[46]C. G. Levi, Curr. Opin. Solid State Mater. Sci. **8**, 77 (2004).